






Distinct phytoplankton assemblages underlie hotspots of primary production in the eastern North Pacific Ocean

Valeria Jimenez ^{1,2} Sebastian Sudek,³ Charlotte Eckmann ^{1,4} Charles Bachy ^{2,5} Camille Poirier,² Fabian Wittmers,^{2,4} Alyson E. Santoro ⁶ Michael J. Follows,⁷ Francisco P. Chavez,³ Irina Shilova ^{1*} Alexandra Z. Worden ^{1,2,4*}

¹Department of Ocean Sciences, University of California, Santa Cruz, California, USA

²Ocean EcoSystems Biology Research Unit, GEOMAR Helmholtz Centre for Ocean Research, Kiel, Germany

³Monterey Bay Aquarium Research Institute, Moss Landing, California, USA

⁴Marine Biological Laboratory, Woods Hole, Massachusetts, USA

⁵Sorbonne Université, Station Biologique de Roscoff, RCC, Roscoff, France

⁶Department of Ecology, Evolution & Marine Biology, University of California, Santa Barbara, California, USA

⁷Department of Earth, Atmospheric and Planetary Sciences, Massachusetts Institute of Technology, Cambridge, Massachusetts, USA

Abstract

Marine eastern boundary current ecosystems, such as the California Current System (CCS), involve productive, mesotrophic transition zones. The CCS exhibits highly variable primary production (PP), yet factors driving the variability and underlying phytoplankton communities remain poorly understood. We integrated physico-chemical and biological data from surface waters sampled during 10 CCS expeditions, spanning 13 yr, and resolved regimes with distinct phytoplankton communities. Additional to an oligotrophic regime (OR), mesotrophic waters beyond the coastal area partitioned into Meso-High and Meso-Low regimes, differing in nitrate concentrations and PP. The OR was dominated by *Prochlorococcus* High-Light I (HLI), and eukaryotic phytoplankton were largely predatory mixotrophs. Eukaryotes dominated Meso-Low and Meso-High phytoplankton biomass. Within the Meso-Low, *Pelagomonas calceolata* was important, and *Prochlorococcus* Low-Light I (LLI) rose in prominence. In the Meso-High, the picoprasinophyte *Ostreococcus lucimarinus* was abundant, and *Synechococcus* Clade IV was notable. The Meso-High exhibited the highest PP ($38 \pm 16 \text{ mg C m}^{-3} \text{ d}^{-1}$; $p < 0.01$) and higher growth rates for photosynthetic eukaryotes ($0.84 \pm 0.02 \text{ d}^{-1}$) than for *Prochlorococcus* ($0.61 \pm 0.01 \text{ d}^{-1}$) and *Synechococcus* ($0.31 \pm 0.05 \text{ d}^{-1}$). An experiment simulating seasonal oligotrophic seawater intrusion into the Meso-High resulted in growth rates reaching $1.18 \pm 0.10 \text{ d}^{-1}$ (*O. lucimarinus*), $0.75 \pm 0.21 \text{ d}^{-1}$ (*Prochlorococcus* LLI), and $0.50 \pm 0.04 \text{ d}^{-1}$ (*Synechococcus* EPC2). Thus, variable PP is underpinned by distinct phytoplankton communities across CCS mesotrophic regimes, and their dynamic nature is influenced by the rapidity with which specific taxa respond to changing environmental conditions or possibly transient nutrient release from viral encounters. Future work should assess whether these dynamics are consistent across eastern boundary current ecosystems and over temporal variations.

Marine phytoplankton are responsible for approximately 50% of global primary production (PP; Field et al. 1998; Huang et al. 2021) and are sensitive to both natural perturbations and climate-induced ecosystem changes (Doney et al. 2012; Arteaga and Rousseaux 2023). Shifts in dominant

phytoplankton taxa due to climate change have already been observed in some high latitude regions (Li et al. 2009). At lower latitudes, predicted increases in water temperature and stratification are expected to result in expansion of low nutrient regions and colonization of these areas by oligotrophic

*Correspondence: azworden@mbi.edu; irina.n.shi@gmail.com

Additional Supporting Information may be found in the online version of this article.

This is an open access article under the terms of the [Creative Commons Attribution-NonCommercial](https://creativecommons.org/licenses/by-nc/4.0/) License, which permits use, distribution and reproduction in any medium, provided the original work is properly cited and is not used for commercial purposes.

Author Contribution Statement: AZW, FC, and SS designed and supervised field programs. VJ, IS, and AZW devised the experiments. FC, VJ, SS, IS, AS, and AZW performed field work. VJ, CAE, CB, CP, and FW generated and analyzed data with additional interpretation by CAE, AS, MJF, IS, and AZW. The manuscript was drafted by VJ and AZW with significant input from MJF, AS, CAE, and IS. All authors have approved the submission.

phytoplankton, such as the cyanobacterium *Prochlorococcus* (Flombaum et al. 2013), with likely ramifications for overall PP and marine food chains.

While knowledge of phytoplankton community dynamics in open ocean and nearshore coastal areas is relatively robust (Alexander et al. 2015; Dai et al. 2023; Messié et al. 2023), comprehension of communities in the spatially dynamic transition zones observed in eastern boundary current ecosystems remains limited. However, eastern boundary current regions have disproportionate ecological importance, comprising only 1% of the global ocean by surface area but contributing 5% of marine primary production and supporting ~20% of global fish catch (Messié and Chavez 2015). The eastern North Pacific Ocean California Current System (CCS) connects to a complex transition zone characterized by meandering currents, jets, fronts, and eddies, and is influenced by variations in upwelling strength and penetration of stratified oligotrophic waters (Checkley and Barth 2009; Kessouri et al. 2020). Despite extensive knowledge of the CCS, shifts in phytoplankton communities that might underpin variations in PP are not well understood (Landry et al. 2009; Taylor et al. 2015; Kranz et al. 2020). In the mesotrophic transition zone, nutrient concentrations and supply rates are lower than in coastal upwelling zones. Previous measurements of both PP and phytoplankton growth rates exhibit high variability in these areas (Landry et al. 2009; Li et al. 2010; Taniguchi et al. 2014). This variability, combined with complex physical oceanography, presents challenges for identifying forcing factors and environmental parameters that shape resident phytoplankton communities.

Phytoplankton community composition in the CCS region is best characterized near the coast, where diatoms and dinoflagellates are important (Dupont et al. 2015; Choi et al. 2020; Closset et al. 2021; Abdala et al. 2022). Studies spanning coastal to oligotrophic offshore stations in the CCS region show clear patterns of phytoplankton distributions, with the cyanobacterium *Prochlorococcus* High-Light I (HLI) dominating the more off-shore oligotrophic regions and the cyanobacterium *Synechococcus* becoming more prominent in mesotrophic stations across the transition zone (Sudek et al. 2014; Ribalet et al. 2015; Kolody et al. 2019). Changes in the relative abundances of *Prochlorococcus* and *Synechococcus* ecotypes along mesotrophic sites have also been linked to the strength of upwelling influence in this area. In years with lower upwelling transport offshore, relative abundances of both *Prochlorococcus* ecotypes HLI and low-light I (LLI) were highest, while in years with stronger upwelling, *Prochlorococcus* HLI remained, and *Synechococcus* clades I and IV became dominant (Sudek et al. 2014). Both *Synechococcus* clades I and IV are known to co-occur and are more abundant in colder, mesotrophic waters (Sohm et al. 2015). The *Synechococcus* Eastern Pacific Clade 2 (EPC2) is also important in the mesotrophic region and maintains stable relative abundances that seem to be less affected by temporal differences in the strength of upwelling (Sudek et al. 2014).

Several groups of photosynthetic eukaryotes are prominent in the CCS transition zone. These include picoeukaryotes, particularly the Class II prasinophytes *Ostreococcus lucimarinus* (also termed Clade OI), isolated off the California, USA coast (Worden et al. 2004), and several *Micromonas* and *Bathycoccus* clades (Simmons et al. 2016; Limardo et al. 2017; Kolody et al. 2019). Additionally, the stramenopile alga *Pelagomonas calceolata* exhibits high relative abundances, as do dictyochophytes further offshore (Dupont et al. 2015; Kolody et al. 2019; Choi et al. 2020). How these taxa coalesce and respond via changes in growth and PP during shifts in biotic and abiotic factors encountered in transition zones is not well understood, providing challenges for predicting future scenarios.

To understand factors driving phytoplankton communities and PP in the transition zone, we performed 10 autumn cruises over 13 yr in the eastern North Pacific Ocean that crossed the CCS. Four of these cruises included additional sampling for phytoplankton enumeration, community composition and nutrient measurements, as well as dilution experiments to determine growth rates. Our study reveals that the transition from the edge of the gyre (800 km from shore) toward the coast partitions into three ecological regimes, as identified by physiochemical measurements, phytoplankton communities, and overall PP. The North Pacific Subtropical Gyre populations define an Oligotrophic Regime (OR) which transitions into an intermediate Mesotrophic Low water (Meso-Low) and Mesotrophic High water (Meso-High), both of which are beyond a coastal regime. Nitrate concentrations in these regimes align with early studies of the Mauritanian eastern boundary current system, defining $> 10 \mu\text{M}$ nitrate as eutrophic, ~ 0.5 to $2 \mu\text{M}$ or higher as mesotrophic, and approaching detection limits (typically 3–10 nM) as oligotrophic (Babin et al. 1996; Morel 1996). Here, each regime was characterized by different contributions and growth rates of cyanobacterial and photosynthetic eukaryotic taxa, with nitrate availability appearing to be a key factor. The resulting differentiation of phytoplankton assemblages across these three biomes contribute to observed variations in PP in the CCS.

Materials and methods

Oceanographic sampling

This study integrates data from 10 autumn research expeditions in the Northeastern Pacific Ocean from 2000 to 2013. Seawater was collected from between 0 and 15 m using a CTD Niskin Rosette or, in some cases, a GO-FLO water sampler, at six major stations along CalCOFI line 67 (67–60, 67–65, 67–70, 67–135, 67–145, and 67–155) and coastal Sta. H3, and around these stations when following a drifter (Dataset S1). Nutrient samples (NO_3^- , NO_2^- , PO_4^{3-} , and SiO_4^{4-}) were collected and analyzed as in Pennington and Chavez (2000). Samples for flow cytometry analysis were collected in 2007–2013 and preserved with glutaraldehyde (0.25% final concentration), fixed at room

temperature in the dark for 20 min, flash-frozen in liquid nitrogen, and stored at -80°C until further use. Seawater for DNA sequencing was collected from a subset of samples ($n = 20$), including those from dilution experiments, by filtering 1 L of sample onto $0.2\ \mu\text{m}$ pore size Supor filters (Pall Scientific), which were then frozen and stored at -80°C until further use.

Primary production measurements and dilution experiments

Primary production measurements by the ^{14}C -bicarbonate method (Steemann Nielsen 1952) were performed in most years from 2000 to 2013 from surface samples (5–15 m) using incubators simulating in situ conditions, following Pennington and Chavez (2000). Depth-specific total carbon fixation (expressed as $\text{mg C m}^{-3} \text{d}^{-1}$, i.e., the same as $\mu\text{g C L}^{-1} \text{d}^{-1}$) was estimated for the 100%, 50%, 30%, 15%, 5%, 1%, and 0.1% light penetration depths estimated by Secchi disk following Parsons et al. (1984), with net primary production (NPP) reflecting the average of the 100% and 50% depths.

To determine growth rates and estimate biomass production six dilution experiments were performed with modifications from previous studies (Landry and Hassett 1982; Worden and Binder 2003) as detailed below. Two experiments were conducted at Sta. 155 (in 2009; 155-2009) and Sta. 135 (in 2011; 135-2011). Four experiments were performed at Sta. 70 (in 2009, 2011, and 2013; 70-2009, 70-2011, and 70-2013) and Sta. 60 (in 2012; 60-2012). Incubations were performed in 4 L polycarbonate bottles in on-deck incubators with light and temperature adjusted to that of the station and depth of water collection (5–15 m) using neutral density filters with quantification of photosynthetically active radiation and a heat exchanger/water recirculator, respectively.

All materials used in dilution experiments were acid-cleaned with 4% trace metal clean HCl in MilliQ water. Whole and filtered seawater were distributed to bottles as: 100% whole (undiluted—i.e., with grazers) and 80% filtered ($0.2\ \mu\text{m}$ sterile capsule filters) plus 20% whole (80% filtered—i.e., reduced grazers—providing the minimum growth rate after reducing grazing mortality; see Text S1 for additional details). Treatments were conducted in triplicate except in experiments 70-2011 and 60-2012, where four biological replicates were used. Incubations were performed for 48 h with sampling at the 0, 24, and 48 h timepoints, except for experiments 70-2009 and 135-2011, which were sampled at 0 and 24 h. Sampling occurred just before dawn and bottles were sacrificed at each timepoint.

Additionally, a 70-2011 experiment conducted at Sta. 70 in 2011 evaluated the impact of naturally occurring oligotrophic water intrusion (such as from Sta. 135) into the mesotrophic waters, hereafter referred to as a perturbation experiment. Treatments and controls were performed in quadruplicate and included whole seawater from Sta. 70 (undiluted), 20% whole seawater from Sta. 70 with 80% Sta. 70 diluent ($0.2\ \mu\text{m}$ capsule filter as above; control), 20% whole seawater from Sta. 70 with 80% Sta. 135 diluent (“oligo,” collected and filtered 4 d before

experiment start), or 20% whole seawater from Sta. 70 with 80% Sta. 135 diluent amended with $5\ \mu\text{mol NO}_3^-$ (“oligo + NO_3^- ”).

For all dilution experiments, theoretical true growth rate, in the absence of grazing, and mortality rates were calculated as in Landry and Hassett (1982) using flow cytometry data (see below). For species- or clade-specific growth and mortality calculations an approach was derived from Worden and Binder (2003) using qPCR or flow cytometry data combined with amplicon data (see below). *Prochlorococcus*, *Synechococcus*, and photosynthetic eukaryote biomass production was calculated using equations from (Landry et al. 2000; Cuvelier et al. 2010). For details see Text S1.

Flow cytometry and biomass estimates

Flow cytometry samples collected from the in situ sampling and dilution experiments were analyzed on an Influx flow cytometer (BD Biosciences) as described previously (Cuvelier et al. 2010) (Dataset S1). Fluoresbrite yellow-green $0.75\ \mu\text{m}$ diameter beads (Polysciences Inc.) were used as internal standards. Each sample was run at a rate of $25\ \mu\text{L min}^{-1}$ for 8 min following a 2 min pre-run, with volume determined by weighing. Cytograms were analyzed using WinList 7.0 (Verity Software House). *Prochlorococcus*, *Synechococcus*, and photosynthetic eukaryotes were distinguished based on forward angle light scatter (FALS), chlorophyll-derived red autofluorescence (692/40 nm bandpass), and phycoerythrin-derived orange fluorescence (572/27 nm bandpass) from *Synechococcus*. *Prochlorococcus*, *Synechococcus*, and photosynthetic eukaryote abundances were then used with established carbon conversion factors to estimate biomass, specifically 39, 82, and $530\ \text{fg C cell}^{-1}$, respectively (Worden et al. 2004).

DNA extraction, V1-V2 16S rRNA gene amplicon analyses, and qPCR

DNA was extracted using a protocol modified from the DNeasy Plant Kit (Qiagen; Demir-Hilton et al. 2011) and quantified with the Qubit dsDNA high-sensitivity assay kit (Life Technologies). V1-V2 16S rRNA amplicon sequencing was performed as in Sudek et al. (2014), and detailed in Text S1. Quality control of reads and the amplicons generated—as well as taxonomical classification of amplicons using a maximum likelihood approach and full-length 16S rRNA gene reference alignments via the PhyloAssigner pipeline (v6.166)—were performed as in Choi et al. (2020).

Phytoplankton community composition analyses based on V1-V2 16S rRNA amplicons were performed in a subset of samples ($n = 12$, years 2009, 2011–2013; Dataset S2). Relative abundance of each cyanobacteria taxa was calculated out of the total number of amplicons assigned to cyanobacteria. *Synechococcus* amplicon values were divided by two as the genomes typically contain two copies of the 16S rRNA gene, whereas *Prochlorococcus* genome sequences typically contain one (Fuller et al. 2003; Větrovský and Baldrian 2013). For photosynthetic eukaryotes, relative abundance of each taxon was

calculated relative to the total number of reads assigned to plastid 16S rRNA and calculated out of the total number of reads assigned to each specific alignment/phylogenetic tree: Viridiplantae (green algae), pelagophytes, and dictyochophytes.

Quantitative PCR (qPCR) primer-probe sets specific for *Ostreococcus* Clade OI, *Bathycoccus* (Demir-Hilton et al. 2011), and *P. calceolata* (Choi et al. 2020) were used to quantify 18S rRNA genes from these taxa in the same samples as used for amplicon sequencing, as well as for 2011–2013 dilution experiment samples. Standard curves were generated as described by Demir-Hilton et al. (2011). See Text S1 for details.

Statistical analyses

To compare environmental factors across samples, principal component analysis (PCA) was performed on the physicochemical measurements (temperature, salinity, NO_3^- , NO_2^- , PO_4^{3-} , SiO_4^{4-}) associated with surface seawater samples (0–15 m) using the PCA function in the FactoMineR package with scaling = TRUE (Lê et al. 2008). To group samples according to environmental factors, hierarchical clustering, using Euclidean distance matrix and Ward's minimum variance method for clustering, was performed based on the PCA scores using the HCPC function in FactoMineR. Clusters were validated with a pairwise permutational multivariate ANOVA test (PERMANOVA, permutations = 9999) using Bray–Curtis distance matrix via the pairwiseAdonis function in the vegan package in R (Oksanen et al. 2024). Post clustering, averages were developed for the biological data (as below) according to the regime/cluster in which the samples were placed and statistical differences were determined via *t*-tests using the function `t_test` in R.

Differences in phytoplankton community composition between samples were analyzed using Bray–Curtis distance matrix with Non-metric Multi-dimensional Scaling (NMDS) and analysis of similarities (ANOSIM) test (permutations = 9999) from the R package vegan. Taxonomy input for both analyses was the relative abundances of cyanobacterial clades out of total cyanobacteria 16S rRNA amplicons and eukaryotic taxa out of total plastid amplicon sequences (to the genus and species level where possible). Environmental data (as above) was fitted to NMDS scores with 9999 permutations and Bonferonni correction using the `envfit` function in the R package vegan.

Results

Surface ocean characteristics, phytoplankton abundances, and PP

To characterize phytoplankton communities across an eastern boundary current system, autumn-time cruises were conducted transecting from coastal California to 800 km offshore (Fig. 1a; Dataset S1). The cruises took place between 2000 and 2013, with the most intensive biological sampling (e.g., flow cytometry, sequencing) and dilution experiments performed between 2009 and 2013. Since our goal was to examine phytoplankton community assembly in relation to the

physicochemical parameters, the latter period served as the primary focus. Hierarchical clustering based on PCA of abiotic factors (i.e., nutrient concentrations, temperature, and salinity) in surface waters distinguished four significant clusters ($p < 0.01$, PERMANOVA, $n = 55$; Figs. 1, S1; Dataset S1a). These were coastal (H3 and vicinity), oligotrophic regime (OR, Sta. 135, 145, 155), and two mesotrophic water types, Mesotrophic-Low (Meso-Low) and Mesotrophic-High (Meso-High), that came from Sta. 60 to 70 (as termed herein; see Fig. 1b).

The Meso-High and Meso-Low regions were not fixed geographically but were 96–170 km from shore, based on the sampling herein. At these sites, water densities were relatively consistent, and, like temperature, were differentiated from the coastal zone and OR (Figs. 1b, S1a,b; Dataset S1). NO_3^- concentration averaged $0.07 \pm 0.07 \mu\text{M}$ in OR surface waters, vs. $0.33 \pm 0.23 \mu\text{M}$ and $1.95 \pm 0.69 \mu\text{M}$ in the Meso-Low and Meso-High, respectively. In the Meso-Low, NO_3^- , PO_4^{3-} , and salinity were significantly lower ($p < 0.05$), and temperature was higher ($p < 0.001$) than in the Meso-High (Fig. 1b). Both mesotrophic regimes were significantly different from the coastal cluster which had NO_3^- concentrations $> 6 \mu\text{M}$ and was used only as a reference point for defining offshore waters. Net primary production (NPP) was measured in a subset of samples and was highest in the Meso-High regime ($38 \pm 16 \text{ mg C m}^{-3} \text{ d}^{-1}$, 95% conf. interval, $p < 0.01$, $n = 18$). In the Meso-Low and OR, NPP was $21 \pm 15 \text{ mg C m}^{-3} \text{ d}^{-1}$ ($n = 13$) and $4 \pm 1 \text{ mg C m}^{-3} \text{ d}^{-1}$ ($n = 12$), respectively (Fig. 1c). Thus, both mesotrophic regimes were distinct based on physicochemical parameters from the colder, higher nutrient coastal waters and from the warm, low-nutrient oligotrophic water. The PCA captured 75% of the variation between the 55 samples (Fig. S1c). To develop a more nuanced view, we also analyzed these samples without the coastal data. In this case, PC1, which was most closely associated with NO_3^- , explained 45.7% of the variance that separates Meso-High from Meso-Low and OR (Fig. S1d).

Broad scale physicochemical patterns were mirrored by differences in the phytoplankton community structure. Both absolute abundances and relative contributions of *Prochlorococcus*, *Synechococcus*, and photosynthetic eukaryotes determined by flow cytometry differed across the regimes (Fig. 1d; Dataset S1). *Prochlorococcus* had highest contributions in the OR, averaging $155,180 \pm 23,058 \text{ cells mL}^{-1}$ and comprising $86 \pm 3\%$ of the phytoplankton biomass, followed by photosynthetic eukaryotes ($11 \pm 2\%$). *Synechococcus* had the lowest biomass contributions in the OR ($p < 0.001$) and equivalent biomass contributions ($p > 0.05$) in the Meso-Low ($4.0 \pm 2.4 \text{ mg C m}^{-3}$) and Meso-High ($7.0 \pm 3.1 \text{ mg C m}^{-3}$). The highest photosynthetic eukaryotic biomass was observed in Meso-High, with abundance averaging $37,100 \pm 9171 \text{ cells mL}^{-1}$ and forming $75 \pm 5\%$ of phytoplankton biomass, and $16,283 \pm 5602 \text{ cells mL}^{-1}$ in the Meso-Low ($62 \pm 5\%$ of the phytoplankton biomass). Photosynthetic eukaryotes standing stock biomass (as opposed to relative contributions per sample) was

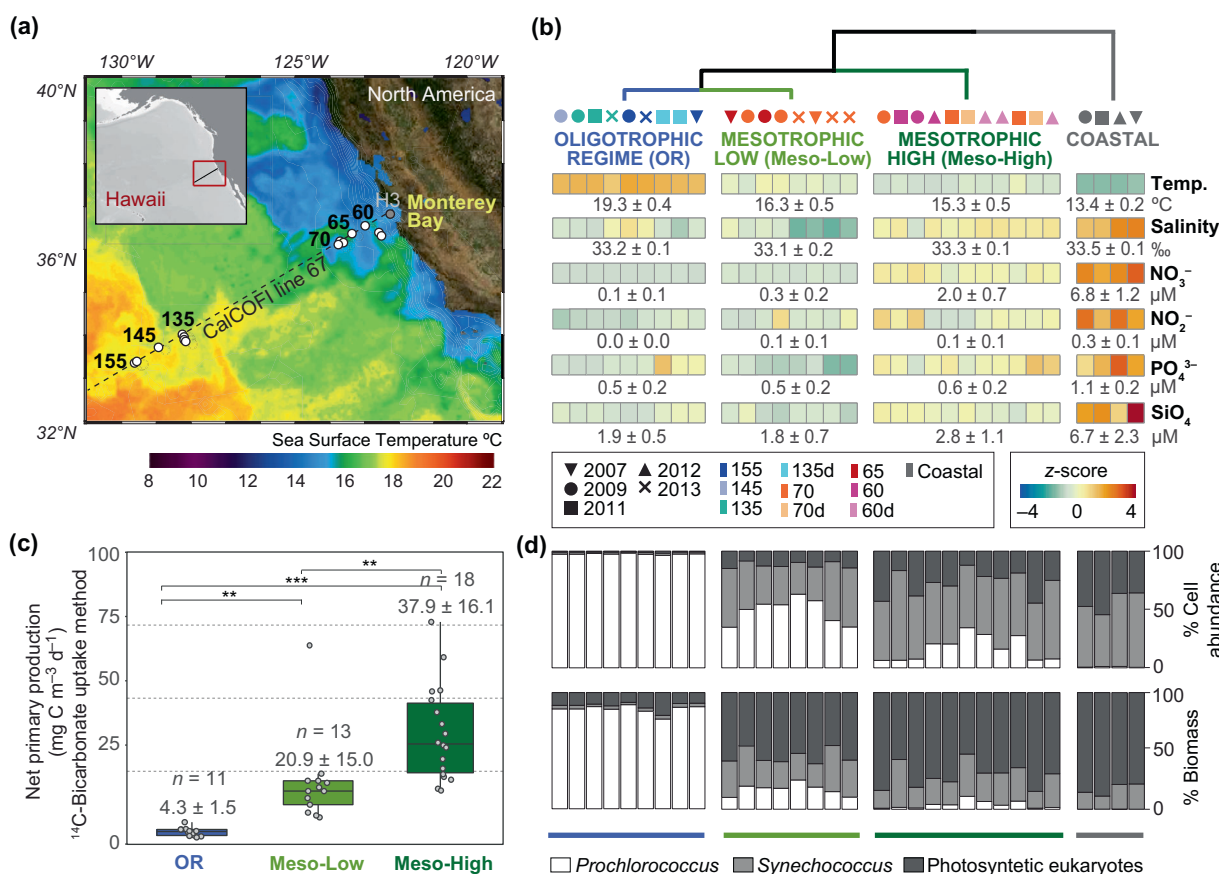


Fig. 1. Distinct regimes in the eastern North Pacific. **(a)** Map of oligotrophic (155, 145, and 135), mesotrophic (70, 65, and 60; both high and low), and coastal (H3) stations correspond to locations of sampling and drifter deployment along line-67 (Pennington et al. 2007) in the eastern North Pacific California Current System (CCS) offshore Monterey Bay, California, USA. The inset shows the location of Line-67 relative to Hawaii. Background shows sea surface temperature from October 2011. **(b)** Average and standard deviation for environmental parameters of surface samples (0–15 m) distinguish four significant ($p < 0.01$) regimes: coastal (shown as a reference, $n = 4$), oligotrophic (OR), Mesotrophic-Low (Meso-Low), and Mesotrophic-High (Meso-High). The heat map reflects the z-score for the indicated sample computed using all 55 samples, shown here only for the subset with corresponding flow cytometry data. Cruise year and stations (or drifters [d]) around station are indicated by shape and color, respectively. The schematic topology of hierarchical clustering reflects the results of the PCA (Fig. S1a). **(c)** Net primary production (^{14}C -Bicarbonate uptake-method) averages and standard deviations per regime. ** $p < 0.01$ and *** $p < 0.0001$ (t-test). **(d)** Cell abundance and estimated biomass contributions of the three major phytoplankton groups based on flow cytometry data.

significantly ($p < 0.001$) greater in both mesotrophic regimes than that of either *Prochlorococcus* or *Synechococcus* in the OR, Meso-Low, and Meso-High (Dataset S1b). Altogether, estimated total phytoplankton biomass declined from $27.6 \pm 5.5 \text{ mg C m}^{-3}$ (Meso-High) to $15.5 \pm 6.2 \text{ mg C m}^{-3}$ (Meso-Low) and $7.0 \pm 1.0 \text{ mg C m}^{-3}$ (OR) ($p < 0.05$).

Phytoplankton community composition

Phytoplankton community composition was characterized in detail using V1-V2 16S rRNA gene amplicons, which allowed identification of cyanobacteria and eukaryotic phytoplankton (based on plastid-derived 16S rRNA gene for the latter). Relative abundances were computed in three ways, depending on the group under consideration: out of total cyanobacterial amplicons, out of total plastid-derived

amplicons, or out of total phytoplankton amplicons (cyanobacterial plus plastid amplicons).

Consistent with flow cytometry data, *Prochlorococcus* dominated in the OR ($91 \pm 2\%$ of total phytoplankton V1-V2 16S rRNA amplicons, Fig. S2a), with *Prochlorococcus* HLI having the highest relative abundance ($98 \pm 0\%$ of cyanobacterial amplicons, Fig. 2a). Photosynthetic eukaryotes were the second most abundant OR group ($7 \pm 2\%$ of total phytoplankton amplicons), out of which stramenopiles dominated ($72 \pm 6\%$ of plastid amplicon abundances; Fig. S2b), largely represented by dictyochophytes (Fig. 2b).

In mesotrophic regimes, *Prochlorococcus* relative abundances decreased significantly compared to the OR ($p < 0.05$), forming $31 \pm 4\%$ in Meso-High (primarily HLI), and $5 \pm 3\%$ in Meso-Low (largely HLI followed by LLI) of total phytoplankton amplicons (Fig. 2a). Relative contributions of *Synechococcus* to

phytoplankton amplicons was not significantly different between the Meso-Low and Meso-High ($15 \pm 2\%$ and $17 \pm 8\%$, respectively) but dominated cell abundance and cyanobacterial amplicons ($75 \pm 4\%$) in Meso-High. In the Meso-Low, *Synechococcus* Clades IV and EPC2 formed $13 \pm 4\%$ and $11 \pm 4\%$ of cyanobacterial amplicons, respectively. In the Meso-High, Clade IV was the most abundant ($56 \pm 14\%$) cyanobacterium, followed by *Synechococcus* Clade I and Clade EPC2 ($10 \pm 2\%$ and $7 \pm 1\%$, respectively). Photosynthetic eukaryotes comprised $40 \pm 0\%$ and $62 \pm 16\%$ of total phytoplankton V1-V2 16S rRNA amplicons in Meso-Low and Meso-High, respectively.

Eukaryotic phytoplankton transitioned from stramenopile dominance of plastid 16S rRNA amplicon relative abundances in the OR ($68.0 \pm 7.2\%$) to prasinophytes in the Meso-High ($64 \pm 10\%$). In the Meso-Low, stramenopiles and green algae contributed $58 \pm 12\%$ and $26 \pm 12\%$, respectively. Highest prymnesiophyte relative abundances occurred in the OR ($17 \pm 6\%$) and decreased in the Meso-Low and Meso-High (Figs. 2b, S2). As expected, diatoms had high relative abundances in the reference coastal sample distinguishing it from the three regimes above (Figs. 2b, S2d).

Due to their prevalence, stramenopiles and green algae were analyzed at higher taxonomic resolution using phylogenetic approaches (Fig. 2b; Text S2). Among stramenopiles, *P. calceolata* dominated mesotrophic regimes, with higher relative abundance in Meso-Low ($32 \pm 7\%$ total plastid amplicons) than Meso-High ($17 \pm 5\%$) (Fig. 2b). Dictyochophytes were more diverse and dominated plastid relative abundances in the OR ($57 \pm 10\%$), where pelagophytes were $< 5\%$. Within green algae, prasinophyte Class VII.B (*Chloroparvula*) had the highest relative abundances in Meso-Low ($19 \pm 11\%$), while Meso-High samples were dominated by prasinophyte Class II ($60 \pm 15\%$), more specifically *Ostreococcus* Clade OI ($52 \pm 18\%$). All *Ostreococcus* amplicons were from *O. lucimarinus*, thus we use the genus species naming henceforth rather than Clade OI.

Phytoplankton community composition was significantly different across the three regimes (ANOSIM, $R = 0.94$ and $p = 0.004$; Fig. S3). Temperature ($R^2 = 0.94$, $p = 0.004$) was the strongest factor separating OR from both Meso-High and Meso-Low, while NO_3^- concentrations separated the two Mesotrophic regimes ($R^2 = 0.72$, $p = 0.038$). Additionally, two approaches were used to verify 16S rRNA amplicon-based inferences about phytoplankton communities. The first compared contributions based on flow cytometric enumeration to relative contributions in 16S rRNA amplicon data. Correlation between contributions of *Prochlorococcus*, *Synechococcus*, and eukaryotes to total phytoplankton amplicons and cell abundances was weaker (Fig. 2c) than correlation to flow cytometry-based biomass estimates (Fig. 2d).

The second approach involved using an absolute method for quantifying the eukaryotic taxa that were identified as

being dominant via relative amplicon abundances in the Meso-Low (*P. calceolata*), and the Meso-High (*O. lucimarinus*), as well as a taxon that was notable in both regimes (*Bathycoccus spp.*). Comparison of the ratios of the two picoprasinophytes enumerated by 18S rRNA qPCR to 16S rRNA amplicon ratios supported patterns seen across regimes via amplicons ($R^2 = 0.88$; Fig. S4b; Datasets S2 and S3; Fig. S4). Additionally, *P. calceolata* had higher qPCR gene counts than the picoprasinophytes in the Meso-Low. All three had higher abundances in the Meso-High than Meso-Low ($p < 0.05$). This was most notable for *O. lucimarinus*, which reached $119,441 \pm 5835$ 18S rDNA gene copies mL^{-1} in the Meso-High, greater than Meso-Low counts by two orders of magnitude.

Phytoplankton growth rates and biomass production

Growth rates and biomass production contributions from *Prochlorococcus*, *Synechococcus*, and photosynthetic eukaryotes were estimated from dilution experiments. All three groups reached their highest growth rates in the Meso-High, with photosynthetic eukaryote growth rates the highest of the three ($0.84 \pm 0.02 \text{ d}^{-1}$), followed by *Prochlorococcus* ($0.63 \pm 0.03 \text{ d}^{-1}$) and *Synechococcus* ($0.46 \pm 0.01 \text{ d}^{-1}$) (Fig. 3a). Grazing mortality was also estimated, with photosynthetic eukaryotes showing the highest average mortality rates, which occurred in the OR and Meso-High (Dataset S4). Grazing mortality was more variable in the Meso-Low, whereas growth rates for all three major phytoplankton groups were most similar to each other in this region.

Next, we estimated *Prochlorococcus*, *Synechococcus*, and photosynthetic eukaryote daily biomass production ($\text{mg C m}^{-3} \text{ d}^{-1}$) using carbon conversion factors for picophytoplankton and the experiment-derived growth rates (Fig. 3b). The greatest overall biomass production ($23 \pm 8 \text{ mg C m}^{-3} \text{ d}^{-1}$) was observed in Meso-High experiments, which was 5 times higher than Meso-Low experiments ($5 \pm 1 \text{ mg C m}^{-3} \text{ d}^{-1}$) and 11 times higher than experiments in oligotrophic waters ($2 \pm 0 \text{ mg C m}^{-3} \text{ d}^{-1}$). In oligotrophic experiments, *Prochlorococcus* accounted for 70% of the total biomass production, and in mesotrophic experiments, photosynthetic eukaryotes accounted for 85% and 73% in Meso-Low and Meso-High experiments, respectively.

In addition to the estimates of growth rates of *Prochlorococcus*, *Synechococcus*, and photosynthetic eukaryotes, species-specific daily growth rates were determined for *O. lucimarinus*, *P. calceolata*, and *Bathycoccus* using qPCR on DNA from mesotrophic regime experiments (Table 1). Growth rates of *O. lucimarinus* and *P. calceolata* increased nearly threefold from the Meso-Low to Meso-High, reaching $0.85 \pm 0.06 \text{ d}^{-1}$ and $0.67 \pm 0.06 \text{ d}^{-1}$, respectively. *Bathycoccus spp.* had the lowest growth rates $< 0.49 \pm 0.01 \text{ d}^{-1}$. All three grew faster in the Meso-High than the Meso-Low, similar to trends observed for the whole eukaryotic phytoplankton community using flow cytometry (Fig. 3).

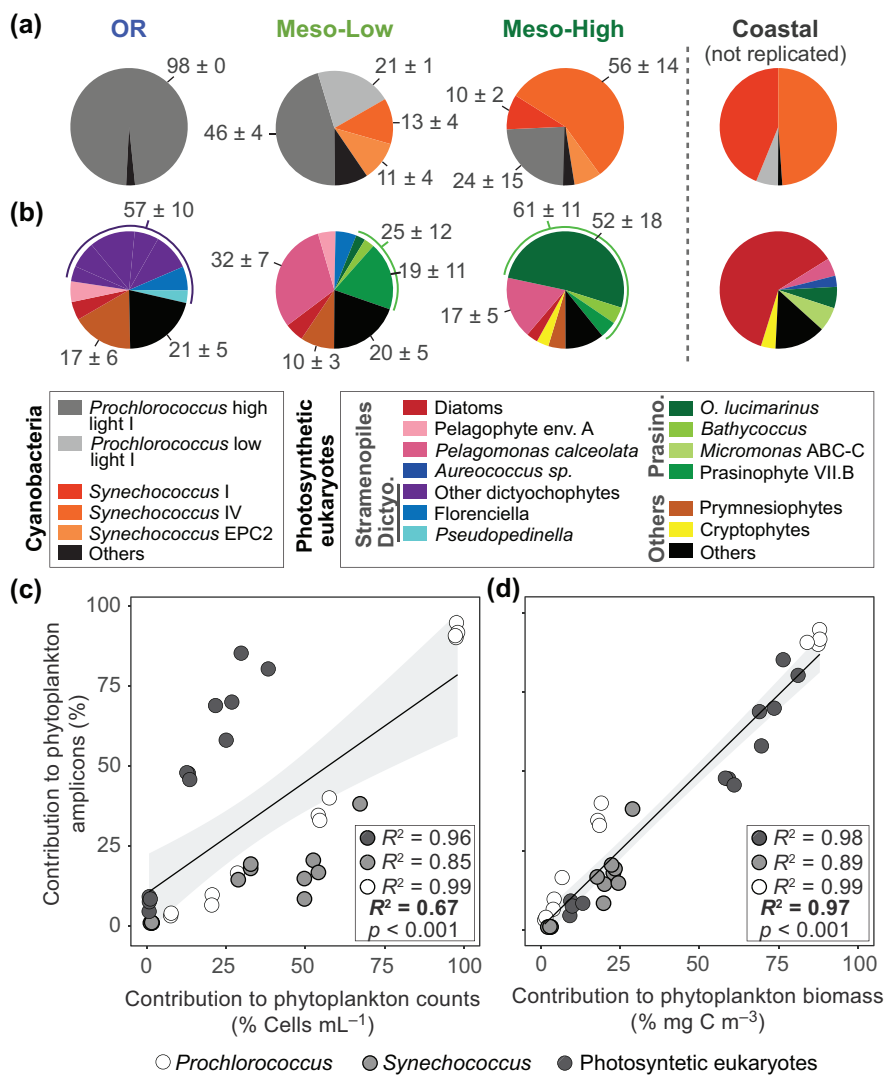


Fig. 2. Phytoplankton assemblages in CCS regimes and relationships between amplicon and flow cytometry data. **(a)** Pie charts representing *Prochlorococcus* and *Synechococcus* ecotype relative abundances computed out of total cyanobacteria V1-V2 16S rRNA gene amplicons. **(b)** Pie charts representing relative abundances (computed out of all plastid V1-V2 16S rRNA gene amplicons) for the most abundant eukaryotic phytoplankton belonging to prasinophyte and stramenopile species and clades, and other major lineages. Taxa with relative abundances averaging < 3% in samples from within a regime are shown as “Others” (including other species of some of the shown genera) in black. Averages ± standard deviations represent data from two different years in each mesotrophic regime and 3 yr in the OR. An unreplicated coastal zone sample depicts common upwelling communities in this system and one mesotrophic sample (Sta. 70, 2009) considered as a transition sample was excluded in this analysis. Note the relative abundance of each green algal taxon (to total plastid amplicons) was < 3% in the OR (and hence not shown). Together green algae accounted for $9.0 \pm 1.2\%$ of OR plastid amplicons. Of these, $2.1 \pm 0.7\%$ putatively assigned to the green algae could not be clearly identified. Also shown is the relationship between contributions of *Prochlorococcus*, *Synechococcus*, and photosynthetic eukaryotes to total phytoplankton 16S rRNA amplicons vs. **(c)** cell abundance by flow cytometry and **(d)** estimated biomass (using flow cytometry data and conversion factors). Result of a linear regression model (R^2 and p -value) are shown for all phytoplankton (bold) and for each group.

Effect of reduced nutrient availability on phytoplankton growth rates

We next simulated the impact of naturally occurring oligotrophic water intrusion into the Meso-High, specifically the effect of mixing in water from the oligotrophic station, where nitrogen concentrations were significantly lower than in mesotrophic stations. NO_3^- was the major factor separating the Meso-High and Meso-Low regimes in our analyses.

Standing stock concentrations of NO_3^- were 5.9 times higher in Meso-High than Meso-Low ($p < 0.05$) and 30 times higher than in the OR (Fig. 1; Dataset S1). Therefore, NO_3^- amendment was also examined in the simulated intrusion to test the hypothesis that nitrogen availability alone affects phytoplankton community composition and growth rates in the CCS (Fig. 4). Water from oligotrophic Sta. 135 ($< 0.01 \mu\text{M NO}_3^-$) was the diluent for Meso-High communities at Sta. 70, both

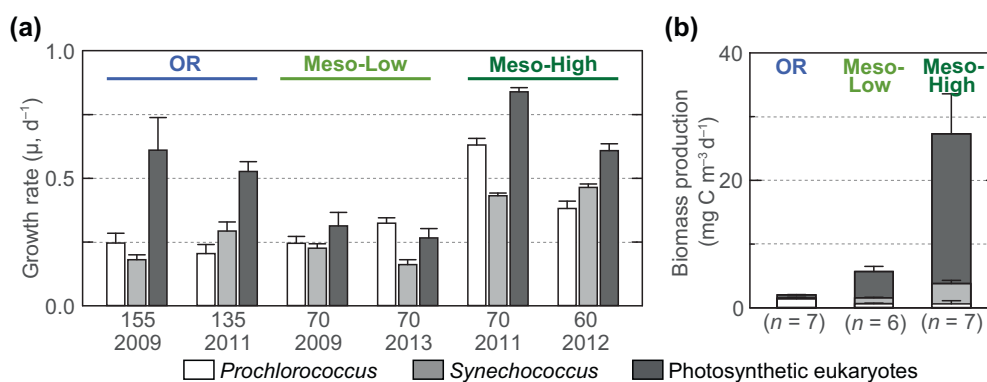


Fig. 3. Growth rates and biomass production in the oligotrophic and mesotrophic regimes of the CCS. **(a)** Dilution experiment-based growth rates via linear regression analysis (theoretical true growth in the absence of grazers; μ , d^{-1}) of *Prochlorococcus*, *Synechococcus*, and photosynthetic eukaryotes, analyzed with flow cytometry, with two oligotrophic experiments and two experiments for each mesotrophic water type. Each experiment was performed in triplicated incubations (except for 70-2011 performed in quadruplicated incubations). Error bars represent the standard error of triplicated or quadruplicated experimental treatments (Dataset S4). **(b)** Dilution experiment-based mean biomass production by *Prochlorococcus*, *Synechococcus*, and photosynthetic eukaryotes ($\text{mg C m}^{-3} \text{d}^{-1}$) in two experiments per regime. The mean and standard deviation (error bars) were calculated from biomass production of all bottles corresponding to the two experiments per regime (so that biological replicates per regime correspond to OR ($n = 7$), Meso-Low ($n = 6$), and Meso-High ($n = 7$)).

with and without NO_3^- amendment, alongside a control (i.e., diluent from Sta. 70).

For the three eukaryotic phytoplankton species examined, growth rates were highest in the oligo + NO_3^- treatment (Fig. 4a; Table 2). *Ostreococcus lucimarinus* and *P. calceolata* had the highest growth rates, 1.18 ± 0.10 and $1.13 \pm 0.15 \text{ d}^{-1}$, respectively, in the oligo + NO_3^- treatment, up to 1.5-fold higher than respective control growth rates. *Pelagomonas calceolata* showed lower growth rates ($0.68 \pm 0.11 \text{ d}^{-1}$) in oligo treatment, whereas for *O. lucimarinus* and *Bathycoccus* lowest growth rates were observed in the control and oligo treatment (Fig. 4a; Table 2).

Table 1. Field growth rates of key picoeukaryote genera and/or species. Rates are given as $\mu \text{ d}^{-1}$ for picoeukaryotes based on qPCR analysis of the 18S rRNA gene in dilution experiments after 48 h incubations. Significance of the linear regression based on model *t*-test is also given with n.s. indicating $p \geq 0.01$.

Regime	Site/yr	Growth rate	Significance
		($\mu \pm \text{SD d}^{-1}$)	$p <$
<i>Ostreococcus lucimarinus</i>			
Meso-low	70/2013	0.54 ± 0.12	0.01
Meso-high	70/2011	1.00 ± 0.06	0.01
Meso-high	60/2012	0.68 ± 0.03	0.05
<i>Bathycoccus spp.</i>			
Meso-low	70/2013	0.29 ± 0.11	0.05
Meso-high	70/2011	0.61 ± 0.07	0.01
Meso-high	60/2012	0.50 ± 0.02	n.s.
<i>Pelagomonas calceolata</i>			
Meso-low	70/2013	0.45 ± 0.10	0.05
Meso-high	70/2011	0.90 ± 0.11	0.01
Meso-high	60,2012	0.76 ± 0.05	0.05

Prochlorococcus HLI was the more abundant *Prochlorococcus* ecotype in this experiment and showed no difference in growth rates between control and oligo, and a slightly higher growth rate in the oligo + NO_3^- treatment (Fig. 4b). The *Prochlorococcus* LLI growth rate was twofold higher in the oligotrophic treatment ($0.75 \pm 0.21 \text{ d}^{-1}$), and slightly more so in the oligo + NO_3^- treatment ($0.85 \pm 0.11 \text{ d}^{-1}$), than the control ($0.36 \pm 0.06 \text{ d}^{-1}$).

Control growth rates for *Synechococcus* Clade IV (the most abundant *Synechococcus* clade in the experiment) also mirrored the flow cytometry-based measurement (Figs. 3, 4c; Table 2). Differences were not observed between treatments for *Synechococcus* Clade I and EPC1, while Clade V/VI/VII growth declined in the oligo treatment compared to the control and oligo + NO_3^- treatment (Fig. 4c; Table 2). In contrast, *Synechococcus* Clade EPC2 did not grow in the control and exhibited higher growth rates in the oligo and oligo + NO_3^- treatments than in the control. Collectively, these results show the distinctive responses of individual ecotypes or species in a simulated push toward a more Meso-Low condition vs. ambient Meso-High conditions.

Discussion

Oceanographic studies have identified areas where high primary productivity occurs, including the eastern boundary current system investigated here (Messié and Chavez 2015; Chavez et al. 2017). Still, data on the activities of specific phytoplankton groups, species, or ecotypes are largely unavailable, despite how evolutionarily and ecologically different these taxa are (Worden et al. 2015). Here, we incorporated data from multiple approaches to investigate phytoplankton communities present in the CCS and how they connect to primary

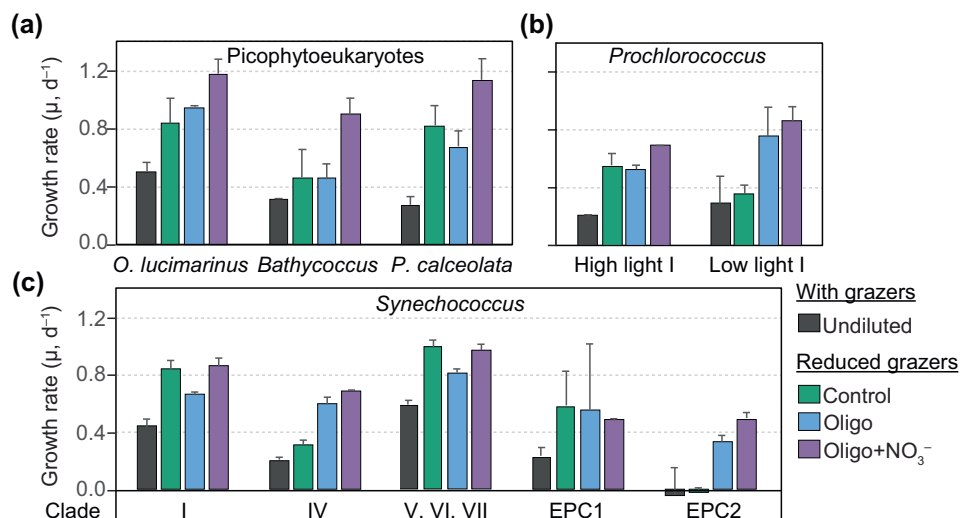


Fig. 4. In situ growth rates of key members of the Meso-High phytoplankton community and responses to oligotrophic water intrusion. Rates for four treatments performed at Sta. 67–70 (2011) over a 24-h period are shown: with grazers (Undiluted; Sta. 70 seawater), and in treatments with reduced grazing pressure (by 80% dilution; i.e., minimum growth rates) with native seawater (control), oligotrophic Sta. 135 water, and oligotrophic water + NO₃⁻ (water amended with 5 μ M NO₃⁻, final concentration) as diluents. Treatments were performed and analyzed in quadruplicate. Growth responses (μ, d^{-1}) based on qPCR are shown for **(a)** *Ostreococcus lucimarinus*, *Bathycoccus* spp., and *Pelagomonas calceolata* using 18S rRNA qPCR data, and **(b)** *Prochlorococcus* and **(c)** *Synechococcus* ecotype growth rates based on V1-V2 16S rRNA amplicons combined with flow cytometry-based cell abundances. Error bars represent the standard deviation, see also Table 2.

production variability in this important region of the eastern North Pacific Ocean. Distinct phytoplankton communities were delineated in offshore CCS surface waters based on abiotic factors, with NO₃⁻ standing stocks appearing to be particularly important to community assembly.

Distinctive offshore regimes in the mesotrophic ocean

Prior measurements of PP in the CCS have been highly variable, with the highest rates often attributed to upwelling. Upwelling is known to provide massive supplies of inorganic nutrients—fueling blooms of diatoms and other

Table 2. Picoplankton responsiveness to perturbation. Specific growth rates for key picoeukaryotic taxa and cyanobacterial ecotypes in the Meso-High (70-2011) under experimentally simulated intrusion of oligotrophic water (and controls). Picoeukaryote rates are based on 18S rRNA gene qPCR analysis (in situ initial cell abundances correspond to mean and error of triplicated qPCR runs). Estimated rates for Cyanobacteria use V1-V2 16S rRNA amplicon data combined with flow cytometry data. For all, the conservative 2-points analysis approach is used (see Methods). The mean and standard deviation of growth rates was calculated from biological duplicates of the quadruplicated treatments.

Species/ecotype	Method	Minimum growth rate (μd^{-1} , 80% diluent)			
		In situ (cells mL ⁻¹)	Control	Oligo diluent	Oligo + NO ₃ ⁻
Picoeukaryotes					
<i>Ostreococcus lucimarinus</i>	qPCR	44,438 ± 1228	0.84 ± 0.17	0.95 ± 0.01	1.18 ± 0.10
<i>Bathycoccus</i>	qPCR	18,838 ± 560	0.46 ± 0.19	0.45 ± 0.11	0.89 ± 0.12
<i>Pelagomonas calceolata</i>	qPCR	11,709 ± 560	0.82 ± 0.14	0.68 ± 0.11	1.13 ± 0.15
<i>Synechococcus</i>					
Clade I	16S/Flow	9327	0.84 ± 0.06	0.66 ± 0.08	0.86 ± 0.06
Clade IV	16S/Flow	61,538	0.32 ± 0.03	0.60 ± 0.02	0.69 ± 0.01
Clade EPC1	16S/Flow	229	0.57 ± 0.26	0.55 ± 0.45	0.48 ± 0.01
Clade EPC2	16S/Flow	10,101	-0.01 ± 0.03	0.33 ± 0.05	0.50 ± 0.04
Clades V/VI/VII	16S/Flow	2221	1.03 ± 0.03	0.81 ± 0.10	0.97 ± 0.02
<i>Prochlorococcus</i>					
Ecotype HLI	16S/Flow	31,353	0.55 ± 0.08	0.53 ± 0.03	0.69 ± 0.01
Ecotype LLI	16S/Flow	1402	0.36 ± 0.06	0.75 ± 0.21	0.85 ± 0.11

algae (Kudela et al. 2006; Kahru et al. 2009; Li et al. 2010; Kranz et al. 2020). Such studies show rates of depth-integrated NPP in the range of 120–718 mmol C m⁻² d⁻¹ (1.44–8.16 g C m⁻² d⁻¹) in coastal and freshly upwelled CCS waters southwards of the region studied here (Kranz et al. 2020). Along Line 67, where our study took place, coastal surface water NPP averaged 140 mg C m⁻³ d⁻¹ at sites shoreward of our mesotrophic transition zones sites (Chavez et al. 2011). Molecular analysis of the same shoreward stations (coastal/~ 8 km from the inner most point of Monterey Bay) showed a predominance of diatoms (Choi et al. 2020), akin to our unreplicated sampling at Sta. H3, 10 km from shore (Fig. 2b). In our study, neither the Meso-Low, nor the Meso-High with its higher NPP (23 ± 8 mg C m⁻³ d⁻¹, albeit lower than coastal values), showed a strong influence of newly upwelled water, which can be tracked via salinity characteristics (Pennington and Chavez 2000). Rather, we found that differentiated communities with significantly different biomass and primary production rates may underpin variability in CCS PP.

High variability in NPP in the core of CCS, offshore from the coastal regime, has been reported before. However, measurements were typically based on chlorophyll concentrations, making it unclear what the biological drivers might be (Munro et al. 2013; Taylor et al. 2015; Kranz et al. 2020). In one such study, NPP ranged between 18 and 48 mmol C m⁻² d⁻¹ with the latter value connecting to waters influenced by wind-stress curl driven upwelling (Kranz et al. 2020). Here, physicochemical characteristics of the Meso-High and Meso-Low regimes were significantly different from each other (Fig. 1). This partitioning was reflected in significant differences in NPP, providing a platform for investigating phytoplankton community assembly. The results point to there effectively being two mesotrophic biomes that are distinct from each other, as well as from classically characterized coastal/upwelling waters and oligotrophic waters.

Transitions in phytoplankton communities from mesotrophic regimes to open ocean

We observed generalized differences across the regimes using phylogenetically parsed 16S rRNA gene amplicon data. Additionally, the results suggest that 16S rRNA amplicon contributions of photosynthetic taxa can serve as a proxy for relative biomass of *Prochlorococcus*, *Synechococcus*, and photosynthetic eukaryotes, at least based on the primers used and populations encountered (generally picoplanktonic) in the offshore waters in the CCS. This analysis showed that *Prochlorococcus* HLI (eMED4) dominated in the OR, as expected based on inferences from prior 16S rRNA amplicon data from the Pacific Ocean (Sudek et al. 2014) and quantitative data from the Atlantic Ocean (Johnson et al. 2006). However, the relative contributions of *Prochlorococcus* to OR phytoplankton abundance and biomass were higher than averaged global *Prochlorococcus* contributions at this latitude (Johnson et al. 2006; Flombaum et al. 2013). This is likely due to the influence of the North

Pacific Subtropical Gyre at our OR sites, which has high *Prochlorococcus* abundances relative to latitudinally similar environments (Karl and Church 2014).

Higher abundance of *Prochlorococcus* LLI (eNATL2A) in the Meso-Low added nuances to reported surface water patterns, that emphasize it has higher abundance than other LL adapted strains as a function of deep photic-zone mixing (Biller et al. 2015). Here, *Prochlorococcus* LLI showed higher growth rates than HLI, specifically in the oligo + NO₃⁻ treatment, potentially in connection to nitrate use (Martiny et al. 2009). In contrast, laboratory growth rates of strains belonging to *Prochlorococcus* HL clades are normally higher than those of LL clades (0.8 and 0.6 d⁻¹, respectively; Zinser et al. 2007; Moore et al. 2007; Biller et al. 2015). The in situ *Prochlorococcus* growth rates in this study region are lower than those reported in warmer, more oligotrophic ecosystems (see Grone et al. 2024 and references therein).

Generally, some *Synechococcus* clade patterns matched prior work from North Pacific oligotrophic and mesotrophic waters, where *Synechococcus* Clades II, III, and X dominated in the oligotrophic open ocean and Clade I and IV dominated in colder, mesotrophic stations (Sohm et al. 2015). However, in our study, *Synechococcus* EPC2 (Sudek et al. 2014) played an important role in defining the Meso-Low, reducing relative contributions of *Synechococcus* clades I and IV (Fig. 2a). Additionally, *Synechococcus* Clade X was found only at low relative abundance (< 0.05%) in the OR. *Synechococcus* biomass production only exceeded that of *Prochlorococcus* in the Meso-High, although having greater standing stock biomass in both Meso regimes (Fig. 1d). This result is consistent with *Synechococcus* being less well adapted to lower nutrient environments than *Prochlorococcus* (Scanlan et al. 2009; Biller et al. 2015).

Most of the major eukaryotic algae in the mesotrophic regimes identified here have been reported in mesotrophic environments, including studies focusing on *Ostreococcus* Clade OI (Demir-Hilton et al. 2011; Clayton et al. 2017; Kolody et al. 2019), prasinophyte Class VII.B (*Chloroparvula*) (Gutiérrez-Rodríguez et al. 2022; Lin et al. 2022), and *Pelagomonas* (Shi et al. 2011; Worden et al. 2012; Dupont et al. 2015). Here, these taxa partition between the regimes, with *Pelagomonas* and prasinophyte Class VII.B relatively more abundant in the Meso-Low and Class II picoprasinophytes, particularly *O. lucimarinus*, dominating in the Meso-High (Fig. 2b).

We also observed specific eukaryotic phytoplankton taxa in the water regimes where they have been rarely documented or have only recently been reported (Choi et al. 2020). For example, pelagophyte Env. Clade A (Choi et al. 2016) was observed in the OR and Meso-Low. Additionally, the dictyochophyte *Florenziella*, a predatory mixotroph (Li et al. 2021) was found in the Meso-Low, and cryptophytes emerged in the Meso-High (Fig. 2b).

In the OR, predatory mixotrophic dictyochophytes were prominent among eukaryotes, as seen in stratified summer surface waters in the Sargasso Sea (Choi et al. 2020). Predatory

phytoplankton have advantages over other eukaryotic phytoplankton in oligotrophic regions because they can avoid direct competition with *Prochlorococcus* for inorganic nutrients by consuming prey (Ward and Follows 2016). The same groups of uncultivated dictyochophytes that were observed herein have recently been shown to consume *Prochlorococcus*, via stable isotope probing (SIP) (Frias-Lopez et al. 2009; Wilken et al. 2023) and cell sorting (Wilken et al. 2019; Choi et al. 2020) studies in the Pacific Ocean.

Finally, contributions from the different genera within Class II prasinophytes showed variations from those in prior eastern boundary current studies from other locations. We note that in contrast to an early report that *Micromonas polaris* can consume bacterial cells (McKie-Krisberg and Sanders 2014), neither *M. polaris*, nor other Class II species that have been examined are capable of predation or predatory mixotrophy (Wilken et al. 2019; Jimenez et al. 2021). Further examination of the initial study results showed that very few cells had been observed, so that statistics could not be performed. Additionally, DAPI-stained dots coinciding with plastids were considered proof of bacterial consumption, although plastids do not contain phagosomes. In the upwelling region off coastal Chile both *Micromonas* and *Ostreococcus* appear to be important (Shi et al. 2009; Rii et al. 2016). Our samples, which lacked a strong signal of upwelling, contained *Micromonas* ABC-C (and less abundant *Micromonas* lineages assigned to the ‘other’ category) but only at low relative abundances. In contrast, *O. lucimarinus* abundance was high in the Meso-High, and *O. lucimarinus* and *Bathycoccus* spp. were present in the Meso-Low, but at lower abundance. Collectively, our results underscore the complexity and variation of eastern boundary current transitions zones, as well as potential seasonal differences that have not been systematically studied.

A highly active picoeukaryotic community underlies Meso-High productivity hotspots

Significantly higher primary and biomass production occurred in the Meso-High than the Meso-Low and OR. *Ostreococcus*, the smallest picoeukaryotic genus known ($\sim 1 \mu\text{m}$ in diameter), was the dominant eukaryotic phytoplankton in the Meso-High, with lower Meso-Low relative abundances. This is surprising given smaller taxa are predicted to have a competitive advantage when inorganic nutrient availability is low due to larger surface area to volume ratios that support nutrient uptake (Chisholm 1992). Presumably, genera with larger cell sizes, for example those at coastal upwelling sites (Choi et al. 2020; Closset et al. 2021), thrive when nutrient availability is high. Here we see larger taxa, although clearly genera that are smaller than those in coastal environments, dominate in the Meso-Low, possibly indicating predatory mixotrophy as a mechanism for nutrient acquisition by prymnesiophytes and uncultivated Pelagophyte Env. Clade A, or potentially uptake of dissolved organic sources (Fig. 2a). Interestingly, *Prochlorococcus*, *Synechococcus*, and picoeukaryotes reached their highest in situ growth rates in the Meso-High

(Fig. 3). The Meso-High community was enriched in *Synechococcus* Clade IV, *O. lucimarinus*, and cryptophytes relative to the OR and Meso-Low, and predatory mixotrophs disappeared (Fig. 2). Overall, rapid phytoplankton growth rates, alongside particularly high picoeukaryote abundances, contributed to high Meso-High PP and biomass production by photosynthetic eukaryotes (Figs. 2b, 3).

Rapid growth of *O. lucimarinus* likely resulted in the high PP observed in the Meso-High regime (Fig. 4a; Table 2). Growth rates reached $1.00 \pm 0.06 \text{ d}^{-1}$ or higher (perturbation experiments, see below) exceeding those from cultures in replete medium with different nitrogen forms (ammonium, nitrate, or urea) in experiments using CCS seawater as a base (Worden et al. 2004). The highest known *O. lucimarinus* laboratory growth rate is $1.52 \pm 0.09 \text{ d}^{-1}$ at 20°C , a higher temperature than in the Meso-High or Meso-Low (Guyon et al. 2018). The results align with data from the northern Chilean eastern boundary current where *Ostreococcus* dominated among picoeukaryotes in stations with higher productivity ($128\text{--}137 \text{ mmol C m}^{-2} \text{ d}^{-1}$ depth integrated PP), *Prochlorococcus* was also important at these stations (Rii et al. 2016). Moreover, frontal regions of the Kuroshio current stimulate high concentrations of *Ostreococcus*, although in that case the more gyre-like *Ostreococcus* Clade OII was the more abundant species (Clayton et al. 2017). In colder waters, during the western North Atlantic bloom, *O. lucimarinus* is one of the dominant phytoplankton (Bolaños et al. 2020). Collectively, these results indicate that this genus is stimulated by dynamic conditions, and that Meso-High regimes elsewhere may well be dominated by *O. lucimarinus*.

Finally, growth rates from the dilution approach generally match those from diel measurements of cell division of cyanobacteria (Worden and Binder 2003), and are considered robust (Landry et al. 2009). It should be noted that losses due to lysis of cells infected by viruses during the experiments could diminish the growth signal from either method. With this caveat in mind, our measurements likely represent minimum growth rates, because viruses of (e.g.) *Bathycoccus* and *Ostreococcus* species have been reported via metagenomics (Kolody et al. 2019) and isolation (Derelle et al. 2006) in CCS waters. Assuming viruses were present, actual in situ growth rates will have exceeded those reported herein. Collectively, stimulation of Class II prasinophytes appears to underpin high Meso-High productivity, and the overall community responsible is different from those that dominate in coastal zones, the OR, and the Meso-Low.

Rapid growth rate changes of specific picophytoplankton lineages under regime shifts

Oligotrophic waters can penetrate inshore in this system, disrupting nutrient and community dynamics (Limardo et al. 2017). Our perturbation experiment simulated this type of intrusion, shifting the Meso-High to a more Meso-Low-like regime, alongside “non-perturbed” controls. Because phosphate concentrations are fairly stable across the regimes

(Fig. 1; Dataset S1; Text S3), the experiment is oriented toward changes in NO_3^- availability which appear to underpin phytoplankton community composition.

Three major phytoplankton response patterns were observed in the perturbation experiments. One generalized response to simulated intrusion of oligotrophic waters was depression of growth rates, likely due to reduced NO_3^- availability. *Pelagomonas calceolata* and *Synechococcus* Clades I and V/VI/VII exhibited this response, while the oligo + NO_3^- treatment restored their growth rates to control levels or higher (Fig. 4). *Pelagomonas calceolata* growth rates were comparable to, or exceeded, the highest culture-based literature value, $0.61 \pm 0.06 \text{ d}^{-1}$ (Dimier et al. 2009). The second response reflected potential benefits of being shifted to conditions more akin to the particular taxon's optimal niche. Growth rates of *Prochlorococcus* LLI and *Synechococcus* Clade EPC2, both of which were more abundant in the Meso-Low than Meso-High, increased markedly with "intrusion" of oligotrophic water.

The third response occurred for *Synechococcus* Clade IV, with growth rates increasing twofold in the oligotrophic intrusion treatments. However, unlike LLI and EPC2, Clade IV was 4-times lower in abundance in the Meso-Low than Meso-High (both by relative abundance and flow cytometry counts adjusted by Clade-specific amplicon data), and the increased growth rates do not appear to reflect response to a more ideal niche. We hypothesize that instead this result may stem from a reduction in encounter rates with Clade-specific phages. As an abundant species in the Meso-High *Synechococcus* Clade IV would presumably be impacted by high encounter rate with its phages, while such phages may largely be absent from the oligotrophic water used as a diluent. If this hypothesis is correct, the growth rates seen under the oligotrophic intrusion simulation represent a "truer" estimate of the in situ growth rate of Clade IV.

Other responses were seen for *Ostreococcus*, *Bathycoccus*, *Prochlorococcus* HLI, and more minor community members. *Ostreococcus lucimarinus* showed similar growth in the control and oligo treatments, and was stimulated (resulting in a growth rate of 1.18 d^{-1}) under the oligo + NO_3^- treatment. *Bathycoccus* spp. and *Prochlorococcus* HLI were largely unaffected by the oligotrophic water "intrusion" and diverged in response to oligo + NO_3^- , with *Bathycoccus* spp. showing a 1.9-fold increase in growth rate, while HLI was only mildly stimulated. Overall, these responses indicate differences in phytoplankton preferences for nitrate availability or shifts in competition for other nutrient sources (e.g., due to the influx of nitrate), or possible influences of differences in taxon-specific phage encounters.

The rapid change in growth rate in response to shifts from Meso-High to (simulated) Meso-Low conditions was especially remarkable. The *Prochlorococcus* LLI growth rate was 2.1 and 2.4-fold (to 0.75 and 0.85 d^{-1}) faster within 24 h in the oligo and oligo + NO_3^- treatments compared to the Meso-High rates. *Synechococcus* EPC2 exhibited negligible growth in

controls and increased to 0.33 and 0.50 d^{-1} in oligo and oligo + NO_3^- treatments. Finally, the 1.4 and 1.9-fold increases in growth rates of the Class II prasinophytes (*O. lucimarinus* and *Bathycoccus* spp., respectively) within 24 h highlight the responsiveness of these organisms to environmental shifts, and likely underpin the decades of research reporting high variability in PP in the mesotrophic ocean.

Conclusions

By integrating data from multiple years, we identify distinct regimes in mesotrophic waters that are not geographically bound and are dynamic in space and time. Collectively, our data indicate that specific Class II prasinophytes are stimulated by Meso-High conditions, leading to high primary production contributions. *O. lucimarinus* dominates in the most productive (Meso-High) regime, whereas in the Meso-Low regime other generally larger eukaryotic phytoplankton are more relatively abundant. Moreover, several taxa—including *Prochlorococcus* LLI and *O. lucimarinus* showed markedly higher growth rates within a day of shifts in water conditions. The identification of distinct regimes highlights that phytoplankton communities respond rapidly to environmental change with shifts in growth rate and community reassembly. This study provides a biological and mechanistic basis for high variability in NPP in the eastern North Pacific transition zone. Future studies will be needed to address how common these regimes are in eastern boundary current systems, potential seasonal and interannual patterns, as well as impacts of changing ocean conditions.

Data availability statement

All data generated and used for this study is provided either in the Datasets S1–S4 which is deposited in figshare (<https://doi.org/10.6084/m9.figshare.c.7466689>) and sequences in the NCBI SRA under accessions SRR26807249–SRR26807261 (BioProject PRJNA1039824).

References

- Abdala, Z. M., S. Clayton, S. V. Einarsson, K. Powell, C. P. Till, T. H. Coale, and P. D. Chappell. 2022. Examining ecological succession of diatoms in California current system cyclonic mesoscale eddies. *Limnol. Oceanogr.* **67**: 2586–2602. doi:10.1002/lno.12224
- Alexander, H., M. Rouco, S. T. Haley, S. T. Wilson, D. M. Karl, and S. T. Dyhrman. 2015. Functional group-specific traits drive phytoplankton dynamics in the oligotrophic ocean. *Proc. Natl. Acad. Sci.* **112**: E5972–E5979. doi:10.1073/pnas.1518165112
- Arteaga, L. A., and C. S. Rousseaux. 2023. Impact of Pacific Ocean heatwaves on phytoplankton community composition. *Commun. Biol.* **6**: 263. doi:10.1038/s42003-023-04645-0

- Babin, M., A. Morel, H. Claustre, A. Bricaud, Z. Kolber, and P. G. Falkowski. 1996. Nitrogen- and irradiance-dependent variations of the maximum quantum yield of carbon fixation in eutrophic, mesotrophic and oligotrophic marine systems. *Deep-Sea Res. I Oceanogr. Res. Pap.* **43**: 1241–1272. doi:10.1016/0967-0637(96)00058-1
- Biller, S. J., P. M. Berube, D. Lindell, and S. W. Chisholm. 2015. *Prochlorococcus*: The structure and function of collective diversity. *Nat. Rev. Microbiol.* **13**: 13–27. doi:10.1038/nrmicro3378
- Bolaños, L. M., and others. 2020. Small phytoplankton dominate western North Atlantic biomass. *ISME J.* **14**: 1663–1674. doi:10.1038/s41396-020-0636-0
- Chavez, F. P., M. Messié, and J. T. Pennington. 2011. Marine primary production in relation to climate variability and change. *Ann. Rev. Mar. Sci.* **3**: 227–260. doi:10.1146/annurev.marine.010908.163917
- Chavez, F., and others. 2017. Climate variability and change: Response of a coastal ocean ecosystem. *Oceanography* **30**: 128–145. doi:10.5670/oceanog.2017.429
- Checkley, D. M., and J. A. Barth. 2009. Patterns and processes in the California current system. *Prog. Oceanogr.* **83**: 49–64. doi:10.1016/j.pocean.2009.07.028
- Chisholm, S. W. 1992. Phytoplankton size. In P. G. Falkowski, A. D. Woodhead, and K. Vivirito [eds.], *Primary productivity and biogeochemical cycles in the sea. Environmental science research*, v. **43**. Springer. doi:10.1007/978-1-4899-0762-2_12
- Choi, D. H., S. M. An, S. Chun, E. C. Yang, K. E. Selph, C. M. Lee, and J. H. Noh. 2016. Dynamic changes in the composition of photosynthetic picoeukaryotes in the northwestern Pacific Ocean revealed by high-throughput tag sequencing of plastid 16S rRNA genes. *FEMS Microbiol. Ecol.* **92**: fiv179. doi:10.1093/femsec/fiv170
- Choi, C. J., and others. 2020. Seasonal and geographical transitions in eukaryotic phytoplankton community structure in the Atlantic and Pacific oceans. *Front. Microbiol.* **11**. doi:10.3389/fmicb.2020.542372
- Clayton, S., Y.-C. Lin, M. J. Follows, and A. Z. Worden. 2017. Co-existence of distinct *Ostreococcus* ecotypes at an oceanic front. *Limnol. Oceanogr.* **62**: 75–88. doi:10.1002/lno.10373
- Closset, I., H. M. McNair, M. A. Brzezinski, J. W. Krause, K. Thamatrakoln, and J. L. Jones. 2021. Diatom response to alterations in upwelling and nutrient dynamics associated with climate forcing in the California current system. *Limnol. Oceanogr.* **66**: 1578–1593. doi:10.1002/lno.11705
- Cuvelier, M. L., and others. 2010. Targeted metagenomics and ecology of globally important uncultured eukaryotic phytoplankton. *Proc. Natl. Acad. Sci. U. S. A.* **107**: 14679–14684. doi:10.1073/pnas.1001665107
- Dai, Y., and others. 2023. Coastal phytoplankton blooms expand and intensify in the 21st century. *Nature* **615**: 280–284. doi:10.1038/s41586-023-05760-y
- Demir-Hilton, E., S. Sudek, M. L. Cuvelier, C. L. Gentemann, J. P. Zehr, and A. Z. Worden. 2011. Global distribution patterns of distinct clades of the photosynthetic picoeukaryote *Ostreococcus*. *ISME J.* **5**: 1095–1107. doi:10.1038/ismej.2010.209
- Derelle, E., and others. 2006. Genome analysis of the smallest free-living eukaryote *Ostreococcus tauri* unveils many unique features. *Proc. Natl. Acad. Sci. U. S. A.* **103**: 11647–11652. doi:10.1073/pnas.0604795103
- Dimier, C., C. Brunet, R. Geider, and J. Raven. 2009. Growth and photoregulation dynamics of the picoeukaryote *Pelagomonas calceolata* in fluctuating light. *Limnol. Oceanogr.* **54**: 823–836. doi:10.4319/lo.2009.54.3.0823
- Doney, S. C., and others. 2012. Climate change impacts on marine ecosystems. *Ann. Rev. Mar. Sci.* **4**: 11–37. doi:10.1146/annurev-marine-041911-111611
- Dupont, C. L., and others. 2015. Genomes and gene expression across light and productivity gradients in eastern subtropical Pacific microbial communities. *ISME J.* **9**: 1076–1092. doi:10.1038/ismej.2014.198
- Field, C. B., M. J. Behrenfeld, J. T. Randerson, and P. Falkowski. 1998. Primary production of the biosphere: Integrating terrestrial and oceanic components. *Science* **1979**: 237–240. doi:10.1126/science.281.5374.237
- Flombaum, P., and others. 2013. Present and future global distributions of the marine cyanobacteria *Prochlorococcus* and *Synechococcus*. *Proc. Natl. Acad. Sci. U. S. A.* **18**: 9824–9829. doi:10.1073/pnas.1307701110
- Frias-Lopez, J., A. Thompson, J. Waldbauer, and S. W. Chisholm. 2009. Use of stable isotope-labelled cells to identify active grazers of picocyanobacteria in ocean surface waters. *Environ. Microbiol.* **11**: 512–525. doi:10.1111/j.1462-2920.2008.01793.x
- Fuller, N. J., D. Marie, F. Partensky, D. Vaultot, A. F. Post, and D. J. Scanlan. 2003. Clade-specific 16S ribosomal DNA oligonucleotides reveal the predominance of a single marine *Synechococcus* clade throughout a stratified water column in the Red Sea. *Appl. Environ. Microbiol.* **69**: 2430–2443. doi:10.1128/AEM.69.5.2430-2443.2003
- Grone, J., C. Poirier, K. Abbott, F. Wittmers, G. S. Jaeger, A. Mahadevan, and A. Z. Worden. 2024. A single *Prochlorococcus* ecotype dominates the tropical bay of Bengal with ultradian growth. *Environ. Microbiol.* **26**: e16605. doi:10.1111/1462-2920.16605
- Gutiérrez-Rodríguez, A., and others. 2022. Planktonic protist diversity across contrasting subtropical and Subantarctic waters of the southwest Pacific. *Prog. Oceanogr.* **206**: 102809. doi:10.1016/j.pocean.2022.102809
- Guyon, J.-B., V. Vergé, P. Schatt, J.-C. Lozano, M. Liennard, and F.-Y. Bouget. 2018. Comparative analysis of culture conditions for the optimization of carotenoid production in several strains of the picoeukaryote *Ostreococcus*. *Mar. Drugs* **16**: 76. doi:10.3390/md16030076
- Huang, Y., D. Nicholson, B. Huang, and N. Cassar. 2021. Global estimates of marine gross primary production based on machine learning upscaling of field observations. *Global*

- Biogeochem. Cycles **35**: e2020GB006718. doi:[10.1029/2020GB006718](https://doi.org/10.1029/2020GB006718)
- Jimenez, V., J. A. Burns, F. Le Gall, F. Not, and D. Vaultot. 2021. No evidence of phago-mixotrophy in *Micromonas polaris* (Mamiellophyceae), the dominant picophytoplankton species in the arctic. *J. Phycol.* **57**: 435–446. doi:[10.1111/jpy.13125](https://doi.org/10.1111/jpy.13125)
- Johnson, Z. I., E. R. Zinser, A. Coe, N. P. McNulty, E. M. Woodward, and S. W. Chisholm. 2006. Niche partitioning among *Prochlorococcus* ecotypes along ocean-scale environmental gradients. *Science* **311**: 1737–1740. doi:[10.1126/science.1118052](https://doi.org/10.1126/science.1118052)
- Kahru, M., R. Kudela, M. Manzano-Sarabia, and B. G. Mitchell. 2009. Trends in primary production in the California current detected with satellite data. *J. Geophys. Res. Oceans* **114**: C02004. doi:[10.1029/2008JC004979](https://doi.org/10.1029/2008JC004979)
- Karl, D. M., and M. J. Church. 2014. Microbial oceanography and the Hawaii Ocean time-series programme. *Nat. Rev. Microbiol.* **12**: 699–713. doi:[10.1038/nrmicro3333](https://doi.org/10.1038/nrmicro3333)
- Kessouri, F., D. Bianchi, L. Renault, J. C. McWilliams, H. Frenzel, and C. A. Deutsch. 2020. Submesoscale currents modulate the seasonal cycle of nutrients and productivity in the California current system. *Global Biogeochem. Cycles* **34**: e2020GB006578. doi:[10.1029/2020GB006578](https://doi.org/10.1029/2020GB006578)
- Kolody, B. C., and others. 2019. Diel transcriptional response of a California current plankton microbiome to light, low iron, and enduring viral infection. *ISME J.* **13**: 2817–2833. doi:[10.1038/s41396-019-0472-2](https://doi.org/10.1038/s41396-019-0472-2)
- Kranz, S. A., S. Wang, T. B. Kelly, M. R. Stukel, R. Goericke, M. R. Landry, and N. Cassar. 2020. Lagrangian studies of marine production: A multimethod assessment of productivity relationships in the California current ecosystem upwelling region. *J. Geophys. Res. Oceans* **125**: e2019JC015984. doi:[10.1029/2019JC015984](https://doi.org/10.1029/2019JC015984)
- Kudela, R. M., W. P. Cochlan, T. D. Peterson, and C. G. Trick. 2006. Impacts on phytoplankton biomass and productivity in the Pacific northwest during the warm ocean conditions of 2005. *Geophys. Res. Lett.* **33**: L22S06. doi:[10.1029/2006GL026772](https://doi.org/10.1029/2006GL026772)
- Landry, M. R., and R. P. Hassett. 1982. Estimating the grazing impact of marine micro-zooplankton. *Mar. Biol.* **67**: 283–288. doi:[10.1007/BF00397668](https://doi.org/10.1007/BF00397668)
- Landry, M. R., J. Constantinou, M. Latasa, S. L. Brown, R. Bidigare, and M. Ondrusek. 2000. Biological response to iron fertilization in the eastern equatorial Pacific (IronEx II). III. Dynamics of phytoplankton growth and microzooplankton grazing. *Mar. Ecol. Prog. Ser.* **201**: 57–72. doi:[10.3354/meps201057](https://doi.org/10.3354/meps201057)
- Landry, M. R., M. D. Ohman, R. Goericke, M. R. Stukel, and K. Tsyrlkevich. 2009. Lagrangian studies of phytoplankton growth and grazing relationships in a coastal upwelling ecosystem off Southern California. *Prog. Oceanogr.* **83**: 208–216. doi:[10.1016/j.pocean.2009.07.026](https://doi.org/10.1016/j.pocean.2009.07.026)
- Lê, S., J. Josse, and F. Husson. 2008. FactoMineR: An R package for multivariate analysis. *J. Stat. Softw.* **25**: 1–18.
- Li, W. K., F. A. McLaughlin, C. Lovejoy, and E. C. Carmack. 2009. Smallest algae thrive as the Arctic Ocean freshens. *Science* **326**: 539. doi:[10.1126/science.1179798](https://doi.org/10.1126/science.1179798)
- Li, Q. P., P. J. S. Franks, M. R. Landry, R. Goericke, and A. G. Taylor. 2010. Modeling phytoplankton growth rates and chlorophyll to carbon ratios in California coastal and pelagic ecosystems. *J. Geophys. Res. Biogeosci.* **115**: G04003. doi:[10.1029/2009JG001111](https://doi.org/10.1029/2009JG001111)
- Li, Q., K. F. Edwards, C. R. Schvarcz, K. E. Selph, and G. F. Steward. 2021. Plasticity in the grazing ecophysiology of *Florenciella* (Dichtyochophyceae), a mixotrophic nanoflagellate that consumes *Prochlorococcus* and other bacteria. *Limnol. Oceanogr.* **66**: 47–60. doi:[10.1002/lno.11585](https://doi.org/10.1002/lno.11585)
- Limardo, A. J., and others. 2017. Quantitative biogeography of picoprasinophytes establishes ecotype distributions and significant contributions to marine phytoplankton. *Environ. Microbiol.* **19**: 3219–3234. doi:[10.1111/1462-2920.13812](https://doi.org/10.1111/1462-2920.13812)
- Lin, Y.-C., C.-P. Chin, W.-T. Chen, C.-T. Huang, G.-C. Gong, K.-P. Chiang, and X.-B. Chen. 2022. The spatial variation in chlorophyte community composition from coastal to offshore waters in a subtropical continental shelf system. *Front. Mar. Sci.* **9**. doi:[10.3389/fmars.2022.865081](https://doi.org/10.3389/fmars.2022.865081)
- Martiny, A. C., S. Kathuria, and P. Berube. 2009. Widespread metabolic potential for nitrite and nitrate assimilation among *Prochlorococcus* ecotypes. *PNAS* **106**: 10787–10792. doi:[10.1073/pnas.0902532106](https://doi.org/10.1073/pnas.0902532106)
- McKie-Krisberg, Z. M., and R. W. Sanders. 2014. Phagotrophy by the picoeukaryotic green alga *micromonas*: Implications for Arctic oceans. *ISME J.* **10**: 1953–1961. doi:[10.1038/ismej.2014.16](https://doi.org/10.1038/ismej.2014.16)
- Messié, M., and F. P. Chavez. 2015. Seasonal regulation of primary production in eastern boundary upwelling systems. *Prog. Oceanogr.* **134**: 1–18. doi:[10.1016/j.pocean.2014.10.011](https://doi.org/10.1016/j.pocean.2014.10.011)
- Messié, M., and others. 2023. Coastal upwelling drives ecosystem temporal variability from the surface to the abyssal seafloor. *Proc. Natl. Acad. Sci.* **120**: e2214567120. doi:[10.1073/pnas.2214567120](https://doi.org/10.1073/pnas.2214567120)
- Moore, L. R., and others. 2007. Culturing the marine cyanobacterium *Prochlorococcus*. *Limnol. Oceanogr.: Methods* **5**: 353–362. doi:[10.4319/lom.2007.5.353](https://doi.org/10.4319/lom.2007.5.353)
- Morel, A. 1996. An ocean flux study in eutrophic, mesotrophic and oligotrophic situations: The EUMELI program. *Deep-Sea Res. I Oceanogr. Res. Pap.* **43**: 1185–1190. doi:[10.1016/0967-0637\(96\)00055-6](https://doi.org/10.1016/0967-0637(96)00055-6)
- Munro, D., P. D. Quay, L. W. Juranek, and R. Goericke. 2013. Biological production rates off the Southern California coast estimated from triple O₂ isotopes and O₂:Ar gas ratios. *Limnol. Oceanogr.* **58**: 1312–1328.
- Oksanen, J., and others. 2024. Vegan: Community ecology package. R package version 2.6-5 [accessed 2023 October 23]. Available from <https://github.com/vegandevs/vegan>

- Parsons, T.R., Maita, Y., Lalli, C.M., 1984. A Manual of Chemical and Biological Methods for Seawater analysis, Pergamon Press, New York. 173pp.
- Pennington, J. T., and F. P. Chavez. 2000. Seasonal fluctuations of temperature, salinity, nitrate, chlorophyll and primary production at Station H3/M1 over 1989–1996 in Monterey Bay, California. *Deep-Sea Res. Part II* **47**: 947–974. doi:[10.1016/S0967-0645\(99\)00132-0](https://doi.org/10.1016/S0967-0645(99)00132-0)
- Pennington, J. T., R. Michisaki, D. Johnston, and F. P. Chavez. 2007. Ocean observing in the Monterey Bay National Marine Sanctuary: CalCOFI and the MBARI time series. Report to the Sanctuary Integrated Monitoring Network (SIMoN).
- Ribalet, F., and others. 2015. Light-driven synchrony of *Prochlorococcus* growth and mortality in the subtropical Pacific gyre. *Proc. Natl. Acad. Sci. U. S. A.* **112**: 8008–8012. doi:[10.1073/pnas.1424279112](https://doi.org/10.1073/pnas.1424279112)
- Rii, Y. M., S. Duhamel, R. R. Bidigare, D. M. Karl, D. J. Repeta, and M. J. Church. 2016. Diversity and productivity of photosynthetic picoeukaryotes in biogeochemically distinct regions of the South East Pacific Ocean. *Limnol. Oceanogr.* **61**: 806–824. doi:[10.1002/lno.10255](https://doi.org/10.1002/lno.10255)
- Scanlan, D. J., and others. 2009. Ecological genomics of marine picocyanobacteria. *Microbiol. Mol. Biol. Rev.* **73**: 249–299. doi:[10.1128/Mmbr.00035-08](https://doi.org/10.1128/Mmbr.00035-08)
- Shi, X. L., D. Marie, L. Jardillier, D. J. Scanlan, and D. Vaultot. 2009. Groups without cultured representatives dominate eukaryotic pico-phytoplankton in the oligotrophic South East Pacific Ocean. *PLoS One* **4**: e7657. doi:[10.1371/journal.pone.0007657](https://doi.org/10.1371/journal.pone.0007657)
- Shi, X. L., C. Lepere, D. J. Scanlan, and D. Vaultot. 2011. Plastid 16S rRNA gene diversity among eukaryotic picophytoplankton sorted by flow cytometry from the South Pacific Ocean. *PLoS One* **6**: e18979. doi:[10.1371/journal.pone.0018979](https://doi.org/10.1371/journal.pone.0018979)
- Simmons, M. P., and others. 2016. Abundance and biogeography of picoprasinophyte ecotypes and other phytoplankton in the eastern North Pacific Ocean. *Appl. Environ. Microbiol.* **82**: 1693–1705. doi:[10.1128/AEM.02730-15](https://doi.org/10.1128/AEM.02730-15)
- Sohm, J. A., N. A. Ahlgren, Z. J. Thomson, C. Williams, J. W. Moffett, M. A. Saito, E. A. Webb, and G. Rocap. 2015. Co-occurring *Synechococcus* ecotypes occupy four major oceanic regimes defined by temperature, macronutrients and iron. *ISME J.* **10**: 333–345. doi:[10.1038/ismej.2015.115](https://doi.org/10.1038/ismej.2015.115)
- Steemann Nielsen, E. 1952. The use of radio-active carbon (C14) for measuring organic production in the sea. *J. Cons.* **18**: 117–140.
- Sudek, S., R. C. Everroad, A. L. Gehman, J. M. Smith, C. L. Poirier, F. P. Chavez, and A. Z. Worden. 2014. Cyanobacterial distributions along a physico-chemical gradient in the North-eastern Pacific Ocean. *Environ. Microbiol.* **17**: 3692–3707. doi:[10.1111/1462-2920.12742](https://doi.org/10.1111/1462-2920.12742)
- Taniguchi, D. A. A., M. R. Landry, P. J. S. Franks, and K. E. Selph. 2014. Size-specific growth and grazing rates for picophytoplankton in coastal and oceanic regions of the eastern Pacific. *Mar. Ecol. Prog. Ser.* **509**: 87–101. doi:[10.3354/meps10895](https://doi.org/10.3354/meps10895)
- Taylor, A. G., M. R. Landry, K. E. Selph, and J. J. Wokuluk. 2015. Temporal and spatial patterns of microbial community biomass and composition in the Southern California Current Ecosystem. *Deep-Sea Res.* **112**: 117–128. doi:[10.1016/j.dsr2.2014.02.006](https://doi.org/10.1016/j.dsr2.2014.02.006)
- Větrovský, T., and Baldrian, P. 2013. The variability of the 16S rRNA gene in bacterial genomes and its consequences for bacterial community analyses. *PLoS One* **8**: e57923. doi:[10.1371/journal.pone.0057923](https://doi.org/10.1371/journal.pone.0057923)
- Ward, B. A., and M. J. Follows. 2016. Marine mixotrophy increases trophic transfer efficiency, mean organism size, and vertical carbon flux. *Proc. Natl. Acad. Sci.* **113**: 2958–2963. doi:[10.1073/pnas.1517118113](https://doi.org/10.1073/pnas.1517118113)
- Wilken, S., and others. 2019. The need to account for cell biology in characterizing predatory mixotrophs in aquatic environments. *Philos. Trans. R. Soc. B: Biol. Sci.* **374**: 20190090. doi:[10.1098/rstb.2019.0090](https://doi.org/10.1098/rstb.2019.0090)
- Wilken, S., C. C. M. Yung, C. Poirier, R. Massana, V. Jimenez, and A. Z. Worden. 2023. Choanoflagellates alongside diverse uncultured predatory protists consume the abundant open-ocean cyanobacterium *Prochlorococcus*. *Proc. Natl. Acad. Sci.* **120**: e2302388120. doi:[10.1073/pnas.2302388120](https://doi.org/10.1073/pnas.2302388120)
- Worden, A. Z., and B. J. Binder. 2003. Application of dilution experiments for measuring growth and mortality rates among *Prochlorococcus* and *Synechococcus* populations in oligotrophic environments. *Aquat. Microb. Ecol.* **30**: 159–174. doi:[10.3354/ame030159](https://doi.org/10.3354/ame030159)
- Worden, A. Z., J. K. Nolan, and B. Palenik. 2004. Assessing the dynamics and ecology of marine picophytoplankton: The importance of the eukaryotic component. *Limnol. Oceanogr.* **49**: 168–179. doi:[10.4319/lo.2004.49.1.0168](https://doi.org/10.4319/lo.2004.49.1.0168)
- Worden, A. Z., J. Janouskovec, D. McRose, A. Engman, R. M. Welsh, S. Malfatti, S. G. Tringe, and P. J. Keeling. 2012. Global distribution of a wild alga revealed by targeted metagenomics. *Curr. Biol.* **22**: R675–R677. doi:[10.1016/j.cub.2012.07.054](https://doi.org/10.1016/j.cub.2012.07.054)
- Worden, A. Z., M. J. Follows, S. J. Giovannoni, S. Wilken, A. E. Zimmerman, and P. J. Keeling. 2015. Rethinking the marine carbon cycle: Factoring in the multifarious lifestyles of microbes. *Science (1979)* **347**: 1257594. doi:[10.1126/science.1257594](https://doi.org/10.1126/science.1257594)
- Zinser, E. R., Z. I. Johnson, A. Coe, E. Karaca, D. Veneziano, and S. W. Chisholm. 2007. Influence of light and temperature on *Prochlorococcus* ecotype distributions in the Atlantic Ocean. *Limnol. Oceanogr.* **52**: 2205–2220. doi:[10.4319/lo.2007.52.5.2205](https://doi.org/10.4319/lo.2007.52.5.2205)

Acknowledgments

We thank the *R/V Western Flyer* captains and crews, especially L Wardle. We thank L Bird for constructing and optimizing temperature-regulated incubators and K Johnson, J Plant, M Blum, E Demir-Hilton, D McRose, N Okamoto, T Pennington, MP Simmons, L Deng, J Robidart, and S Wilken for assistance at sea. Fulbright and CONICYT Fellowships

supported VJ as well as by the National Science Foundation (NSF IOS 0843119 to AZW) and Simons Foundation International (BIOS-SCOPE, to AZW). This research was supported by the David and Lucile Packard Foundation and Gordon and Betty Moore Foundation grant GBMF3788 (to AZW).

Submitted 05 December 2023

Revised 20 June 2024

Accepted 29 November 2024

Associate editor: Osvaldo Ulloa

Conflict of Interest

None declared.